Influence of *m*-isopropenyl-α,α-dimethylbenzyl isocyanate and styrene on non-isothermal crystallization behavior of polypropylene

LiChun Ma · LiPing Li · ChuiGen Guo

Abstract Non-isothermal crystallization kinetics of polypropylene (PP), *m*-isopropenyl-α,α-dimethyl-benzyl isocyanate grafted PP (PP-g-*m*-TMI), and styrene(St), as comonomer, together with *m*-TMI grafted PP (PP-g-(St-*m*-TMI)) was investigated by using differential scanning calorimetry (DSC) under different cooling rates. The crystallization rates of all samples increased with increasing cooling rate. The relation of the half time of crystallization ($t_{1/2}$) of the three samples, $t_{1/2(\text{PP-g-(St-}m\text{-TMI))}} < t_{1/2(\text{PP-g-}m\text{-TMI})} < t_{1/2(\text{PP})}$, implying the introduction of St could effectively improve the degree of grafting of *m*-TMI, resulting in crystallization temperature increased, and the crystallization rate was the fastest. Three methods, namely, the Avrami, the Ozawa, and the Mo, were used to describe the crystallization process of the three samples under non-isothermal conditions. The Avrami and Ozawa neglected the secondary crystallization that follows primary crystallization. The Mo method can successfully describe the overall non-isothermal crystallization process of all the samples. It has been found that the $F(T)_{(\text{PP-g-(St-}m\text{-TMI))}} < F(T)_{(\text{PP-g-}m\text{-TMI})} < F(T)_{(\text{PP})}$, also meaning that the crystallization rate of PP-g-(St-*m*-TMI) and PP-g-*m*-TMI were faster than that of PP. The activation energy (ΔE) for non-isothermal crystallization of all samples was determined by using the Kissinger method. The result showed that the lower value of ΔE for crystallization obtained for PP-g-*m*-TMI and PP-g-(St-*m*-TMI) confirmed the nucleating effect of St and *m*-TMI on crystallization of PP.

Keywords Polypropylene · *m*-TMI · Non-isothermal · Crystallization · DSC

L. Ma · L. Li · C. Guo (✉)
Heilongjiang Key Laboratory of Molecular Design and
Preparation of Flame Retarded Materials, College of Science,
Northeast Forestry University, Harbin 150040, China
e-mail: guochuigen@nefu.edu.cn

C. Guo
MOE Key Laboratory of Bio-Based Material Science
and Technology, Northeast Forestry University,
Harbin 150040, China

Introduction

The physical properties of semi-crystalline polymeric materials strongly depend on their microstructure and crystallinity, because failure of the materials takes place at the microscopic level. The crystalline form can be obtained by slowly cooling the melt or by isothermal crystallization at a temperature between the crystalline melting point and the glass transition temperature [1]. Polypropylene (PP) is a semi-crystalline thermoplastic polymeric material that has been widely used because of its attractive combination of good process ability, mechanical properties, chemical resistance, thermal and thermooxidative stability [2]. However, its inadequate stiffness and brittleness limits its versatile application to some extent [3, 4]. The range of applications can be broadened by improving the adhesion or reactivity of PP. This aim can be reached by introducing polar groups onto the PP backbone. Well-known examples for this are the grafting of maleic anhydride onto PP and the copolymerization of propylene with vinylic monomers [5].

m-Isopropenyl-α,α-dimethylbenzyl isocyanate (*m*-TMI) is a monomer which can also be grafted onto the PP backbone [6, 7]. The reactivity of the isocyanate group makes it a very interesting modifying agent for PP, which has been widely used for in situ or reactive compatibilization. In addition, during the grafting process, styrene

(St), as comonomer, was firstly grafted onto PP, then *m*-TMI was grafted onto the free radical of St, St can increase the grafting yields and reduce the degradation of PP [8]. Therefore, the research has been increasing attention. The *m*-isopropenyl-α,α-dimethyl-benzyl isocyanate grafted PP (PP-g-*m*-TMI) and *m*-TMI grafted PP (PP-g-(St-*m*-TMI)) in this article will be used as interface compatibilizer of the PP/wood flour composites, which can significantly improve the mechanical properties of the PP/wood flour composite [9, 10].

The crystallization behavior of the interface compatibilizer may have a major influence on the crystallization of the matrix in the polymer blends and composites, and thereby on the mechanical properties, such as tensile and impact strength. Additionally, it is well known that polymer and its composites usually undergo a non-isothermal crystallization process, especially in practical processing. Therefore, the investigations of the non-isothermal crystallization behavior of polymer and its composites represents an interesting research subject [11], and can be served as a guide for optimizing process conditions and improving the properties of the final products. At present, the research of the crystallization kinetics of interface compatibilizer, especially *m*-TMI grafted polymer has received little attention. Thus, this study was designed to investigate the effects of *m*-TMI and St on the non-isothermal crystallization kinetics of PP and analysis the kinetic parameters, using differential scanning calorimetry (DSC). Furthermore, the kinetics was analyzed by using Avrami, Ozawa, and Mo methods for non-isothermal crystallization. Finally, the activation energy describing the non-isothermal crystallization process was calculated based on Kissinger Method.

Experimental

Raw materials and sample preparation

PP (MFI is 3 g 10 min^{-1}, density is 0.905 g cm^{-3}) was purchased from Sinopec Beijing Yan shan Chemical Corporation(China); *m*-isopropenyl-α,α-dimethylbenzyl isocyanate (*m*-TMI), molecular formula: $C_{13}H_{15}NO$, molecular weight: 201.3, colorless, transparent liquid, boiling point 543 K, the density: 1.01 g mL^{-1}, provided by Cytec. For preparation: PP-g-*m*-TMI and PP-g-(St-*m*-TMI) were synthesized by melt grafting proportional with PP, *m*-TMI, DCP, St in the mixing chamber of a torque rheometer (RM-200A) operated at 458 K and 60 rpm for 10 min. The concentrations used were 40/3.2/0.2 (by wt%) for PP/*m*-TMI/DCP and 40/3.2/2.7/0.2 (by wt%) for PP/*m*-TMI/St/DCP, respectively. For purification: the reaction mixtures were dissolved in refluxing xylene and hot filtered, the

filtered liquor was washed with acetone for three times, and then the precipitated polymer were dried in vacuum at 363 K. The purified grafted copolymer was white and powdery.

DSC analysis

Non-isothermal crystallization was carried out in the sample pan of a Perkin-Elmer Diamond Differential Scanning Calorimeter, instrument's operating temperature were calibrated with indium. The standard process is as follows: the samples (about 5 mg) were heated from 293 to 463 K with heating rate 150 K min^{-1}, maintained for 5 min in order to eliminate thermal history, then they were cooled at a constant cooling rates of 5, 10, 15, 20, and 30 K min^{-1}, respectively. All the experiments were carried out under pure nitrogen.

Results and discussion

The effects of *m*-TMI and St on the crystallization behavior of PP were analyzed through DSC experiments. Figure 1 shows the crystallization curves of three samples at selected cooling rates of 5, 10, 15, 20, and 30 K min^{-1}, respectively. The crystallization peak temperature (T_p), the crystallization enthalpy (ΔH_c), and the half time of the crystallization ($t_{1/2}$) are listed in Table 1.

Figure 1 and Table 1 show the relationships between T_p and cooling rate (Φ) for PP, PP-g-*m*-TMI, and PP-g-(St-*m*-TMI). For all the samples, the crystallization peak become

Table 1 Kinetic parameters during non-isothermal crystallization process

Sample	Φ/K min^{-1}	T_p/K	$-\Delta H_c$/J g^{-1}	$t_{1/2}$/min
PP	5	389.80	110.502	0.938
	10	386.76	106.926	0.570
	15	384.26	111.018	0.419
	20	382.38	109.396	0.332
	30	378.87	101.193	0.249
PP-g-*m*-TMI	5	391.68	59.206	0.766
	10	387.82	60.772	0.414
	15	385.46	60.340	0.266
	20	383.79	61.434	0.197
	30	381.43	61.987	0.134
PP-g-(St-*m*-TMI)	5	396.83	94.583	0.670
	10	392.61	92.952	0.388
	15	389.83	89.497	0.285
	20	387.79	95.256	0.239
	30	384.57	96.540	0.179

Fig. 1 DSC curves of a PP, b PP-g-*m*-TMI and c PP-g-(St-*m*-TMI) at different cooling rates
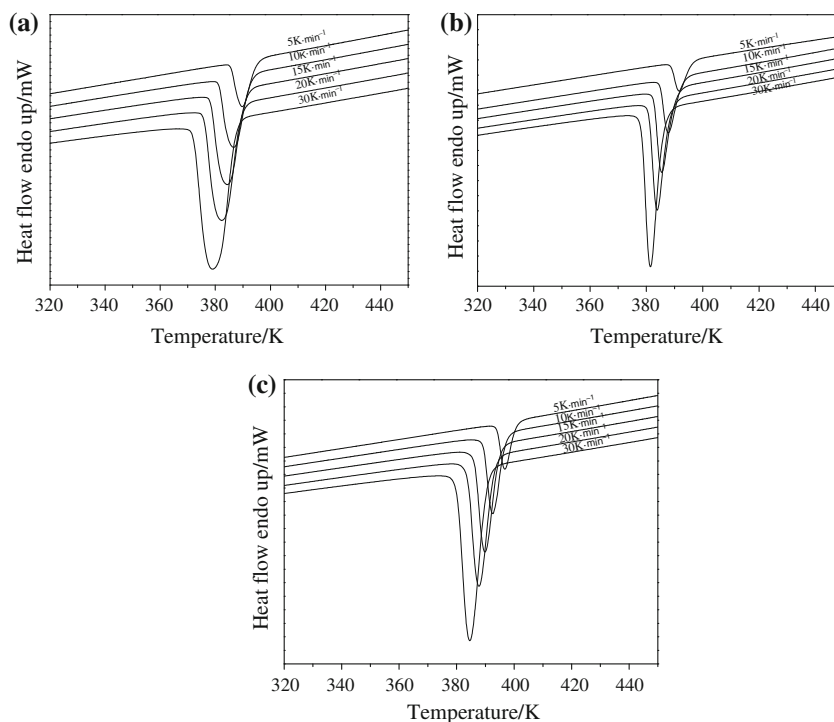
broader and shift to lower temperature with increasing cooling rate. The T_p shift to lower temperature, indicating that at lower cooling rate, the crystallization occurs earlier. When the samples are cooled quickly from the melt, the motion of PP chains cannot follow the cooling rate, because there is not more time to overcome the nucleation energy barrier, crystallization starts at lower temperature [12], therefore, more super cooling is required to initiate crystallization at higher cooling rate. In addition, the nuclei activation is limited and the process of nucleation will consume more time, so that the profile of the crystallization peaks become wider.

In addition, at a given cooling rate (10 K min^{-1}), the T_p increases apparently after grafting *m*-TMI and St onto the PP, which is shown in Fig. 2. On the one hand, it seems that the PP-g-*m*-TMI produces the branched-chain and changes the polarity of PP, which enhances the interaction between PP molecules. Meanwhile, the introduction of *m*-TMI reduces the interface free energy of PP nucleation, and furthermore promotes the crystallization of the PP heterogeneous nucleation [13], thereby increases the crystallization point. On the other hand, during the grafting process, the degradation of PP reduces the entanglement among molecules and increases the regular of PP, so that the crystallization of PP molecular becomes easier. Simultaneously, we can see that the crystallization temperature moves to higher after adding St, it is attributed to the introduction of St that can effectively improve the grafting yields of *m*-TMI. The higher the content of grafted *m*-TMI is, the stronger the
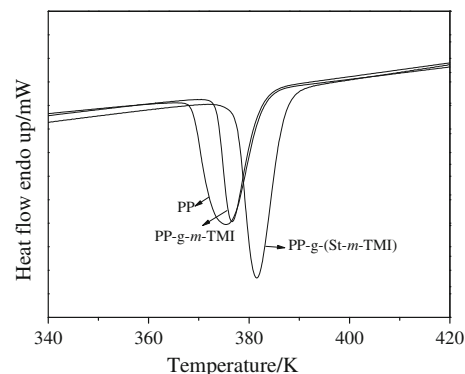

Fig. 2 DSC curves of PP, PP-g-*m*-TMI and PP-g-(St-*m*-TMI) at 10 K min^{-1}

polarity of PP is, which will decrease the interfacial free energy and promote heterogeneous nucleation crystallization of PP. Moreover, the addition of St inhibits the degradation of PP [14], which makes the crystallization temperature drop. However, this decrease of the crystallization temperature would not impact the increase of the temperature in general, namely, integrating the two factors, the former takes much more important roles in the process. Therefore, the crystallization point rises eventually.

The determination of the absolute crystallinity is not required for the analysis of crystallization kinetics, and the relative crystallinity $X(t)$ as a function of crystallization temperature is defined as:

$$X(t) = \frac{\int_{T_0}^{T_t} (dH_c/dT)dT}{\int_{T_0}^{T_\infty} (dH_c/dT)dT} \quad (1)$$

where T_0 is the initial crystallization temperature, T_t and T_∞ are the crystallization temperature at time t and the ultimate crystallization temperatures, respectively. The dH_c is the enthalpy of crystallization released during an infinitesimal temperature range dT. According to different cooling rate (Φ), the temperature parameters can be converted into a timescale by using Eq. 2:

$$t = \frac{T_0 - T_t}{\Phi} \quad (2)$$

where T_t is the crystallization temperature at time t, T_0 is the initial temperature when crystallization begins ($t = 0$), and Φ is the cooling rate. It is notable from Fig. 1 that the values of T_0 under different cooling rates are not the same because of a rate-dependent induction time preceding the initiation of crystallization. From Fig. 1, T_0 increases with a decrease in the cooling rate. According to Eq. 2, the value of T can be transformed into crystallisation time t, as shown in Fig. 3. It shows that the higher the cooling rate is, the shorter the time for completing crystallisation is. Figure 3a–c shows the change in the relative crystallinity $X(t)$ of PP and its grafted product with time t at different cooling rates. All the curves have the same characteristic sigmoid shape. This is caused by the lag effect of the cooling rate during the crystallization process.

Furthermore, an important parameter that can be obtained is the half time of non-isothermal crystallization ($t_{1/2}$), which is the value of the time from the onset of crystallization to the time at which $X(t)$ is 50%, can be obtained from the following relationship:

$$t_{1/2} = \frac{T_0 - T_{1/2}}{\Phi} \quad (3)$$

where $T_{1/2}$ is the crystallization temperature corresponding to the relative crystallinity of 50%. The values of $t_{1/2}$ for PP, PP-g-m-TMI, and PP-g-(St-m-TMI) are also listed in Table 1. It is clear that in the case of the same cooling rate, $t_{1/2 \ (\text{PP-g-(St-}m\text{-TMI))}} < t_{1/2(\text{PP-g-}m\text{-TMI})} < t_{1/2(\text{PP})}$, signifying that the grafting of m-TMI and St could accelerate the overall crystallization process. The results can be explained as follows: the crystallization of PP-g-m-TMI and PP-g-(St-m-TMI) proceeds mainly via heterogeneous nucleation, while that of PP may precede both by heterogeneous and homogeneous nucleation mechanisms. Since homogeneous nucleation starts spontaneously by chain aggregation below the melting point, it requires a longer time, whereas heterogeneous nuclei form simultaneously as soon as the sample reaches the crystallization temperature [15]. Thus, the time to reach the certain crystallinity in grafted PP is shorter than that in PP. At the same time, the m-TMI molecular can act as a heterogeneous nucleating agent due to it is a small molecular to facilitate crystallization and further retrench the time of polymer crystallization. And after adding St, the grafts of St-m-TMI reduced the

Fig. 3 Plots of $X(t)$ versus t of **a** PP, **b** PP-g-m-TMI and **c** PP-g-(St-m-TMI) at different cooling rates
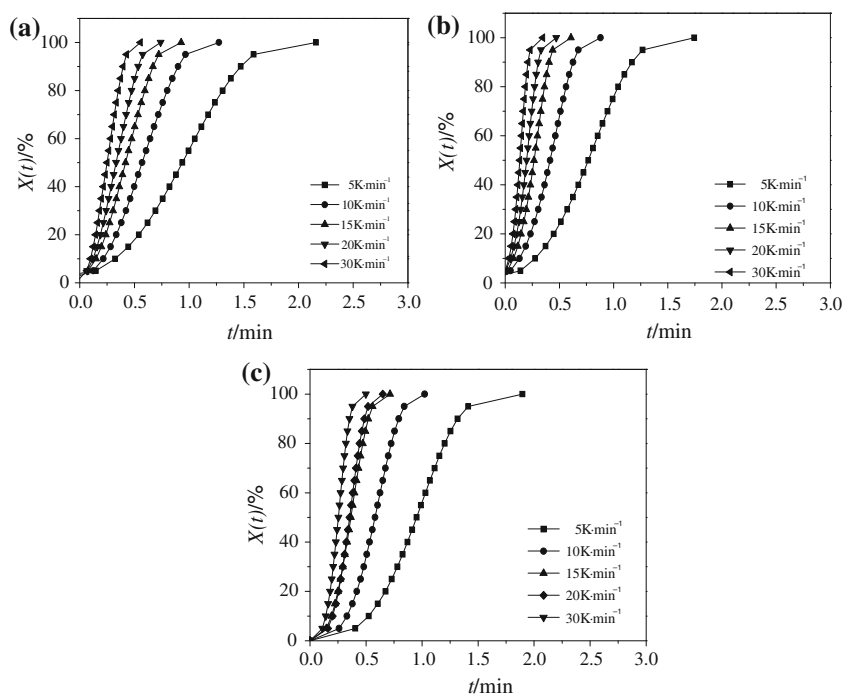
interfacial free energy of crystal nuclei and promoted the heterogeneous nucleating, the value of $t_{1/2}$ becomes the smallest, the reasons can be interpreted as: St and m-TMI are grafted to PP chain possibly in the form of alternating copolymerization, the same phenomenon were reported in other systems [16, 17]. This form promotes the regular spread of polymer molecular chain and accelerates the speed of chain segment migration, so that it reduces the crystal defects and improves the degree of crystallization, further makes PP-g-(St-m-TMI) easier for crystallization.

Several kinetic methods for describing the crystallization behavior of polymers are based on the well-known Avrami equation [18], which can be written as:

$$1 - X(t) = \exp(-k\,t^n). \tag{4}$$

The logarithmic form of Eq. 4 is Eq. 5:

$$\log[-\ln(1 - X(t))] = \log k + n \log t \tag{5}$$

where the Avrami exponent n is a mechanism constant, which depends on the type of nucleation and growth; the parameter k is a rate constant involving both nucleation and growth rate. Parameters n and k have an explicit physical meaning for isothermal crystallization, but for non-isothermal crystallization, their physical meaning does not have the same significance, due to the constant change in temperature [19]. Thus, this must affect both the nucleation and crystal growth processes since they are both temperature dependent.

Figure 4 shows the plots of $\log[-\ln(1 - X(t))]$ versus $\log t$ for crystallization of PP, PP-g-m-TMI, and PP-g-(St-m-TMI) at various cooling rates. It can be seen that the

Table 2 Results of the Avrami analysis for non-isothermal crystallization of PP, PP-g-m-TMI and PP-g-(St-m-TMI)

Φ/K min^{-1}	PP		PP-g-m-TMI		PP-g-(St-m-TMI)	
	n	k/min^{-n}	n	k/min^{-n}	n	k/min^{-n}
5	1.98	0.81	2.06	1.24	2.05	1.63
10	2.09	2.28	1.89	3.79	2.03	4.86
15	1.98	3.94	1.76	7.43	2.17	10.81
20	1.98	6.34	1.64	10.33	2.08	13.88
30	2.10	13.00	1.64	19.41	2.10	26.61

each curve exhibits almost linear relationship. However, each curve shows slight deviation at the end stage of crystallization, the deviation is probably attributable to secondary crystallization, which is caused by the slower crystallization and further perfection of crystals in the later stage [9]. Therefore, Avrami analysis does not effectively describe the overall non-isothermal crystallization of PP, PP-g-m-TMI, and PP-g-(St-m-TMI).

However, the kinetic data in the primary stage can be used to estimate the Avrami parameters for non-isothermal crystallization of the three samples. The values of n and k determined from the slopes and the intercepts of the solid lines (Fig. 4) are listed in Table 2.

The average values of the Avrami exponent are $n = 2.03$, 1.80, and 2.09 for PP, PP-g-m-TMI, and PP-g-(St-m-TMI), respectively. The results indicate that the primary crystallization stage may correspond to a two-dimensional growth of lamellar crystals with thermal nucleation kinetics for non-isothermal melting process of

Fig. 4 Avrami plots of $\log[-\ln(1 - X(t))]$ versus $\log t$ for crystallization of **a** PP, **b** PP-g-m-TMI and **c** PP-g-(St-m-TMI) at different cooling rates
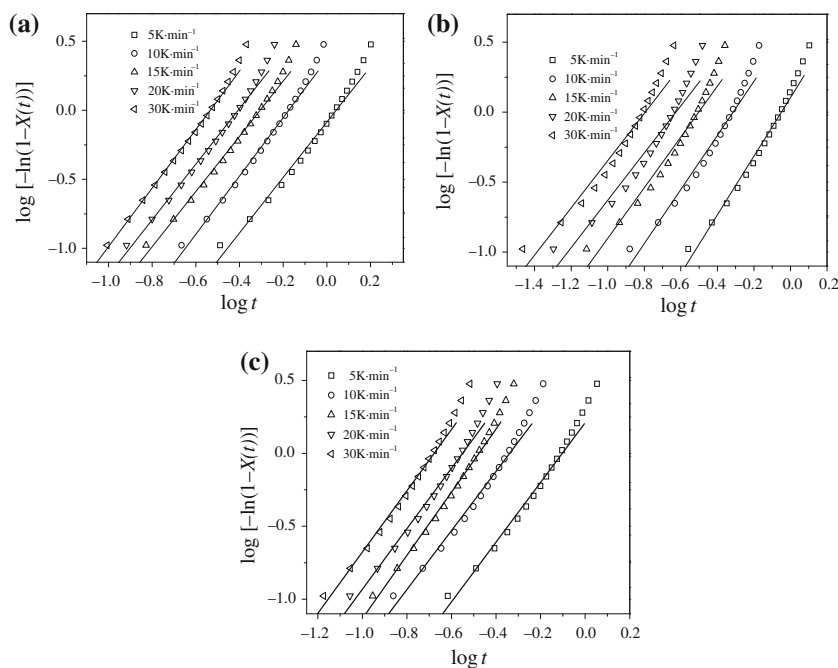
the three samples [16, 20]. Additionally, it is of great interest to compare the Avrami exponent *n* of PP, it is usually reported that the values of the Avrami exponent *n* obtained from DSC are in the ranges of 2–4 [21–24]. The values of *n* in general are influenced by the nature of nucleation and molecular weight of polymer as well as the thermal condition [21], at the same time, polypropylene (PP) is a typical example of a polymer whose structure and properties are profoundly dependent on the tacticity or the stereoregularity of the polymeric chains. PP composed of high stereoregular chains (iPP) tends to take the three-dimensional growth mechanism [25]. Therefore, it can be deduced that the stereoregular structures have significant effect on the growth mode of polypropylene crystals, and the lower dimension of the PP crystals arises from PP has lower tacticity in our experiment.

In addition, the values of *k* increase with increasing cooling rate for PP, PP-g-*m*-TMI, and PP-g-(St-*m*-TMI). This can be explained as the fact that at higher cooling rate, melt crystallization occurs at lower temperature and thus has higher crystallization rate due to higher undercooling. Furthermore, at a given cooling rate, the values of *k* of PP-g-(St-*m*-TMI) are the greatest, and the values of *k* of PP-g-*m*-TMI are greater than those of PP, specifying that the crystallization rate becomes faster after PP matrix is grafted by *m*-TMI and St.

Considering the non-isothermal crystallization being a rate-dependent process, Ozawa [26] extended the Avrami equation to the non-isothermal condition by replacing time variable in Avrami equation with a variable cooling rate and derived a kinetic equation as follows:

$$1 - X(T) = \exp[-K(T)/\Phi^m] \tag{6}$$

where $X(T)$ is relative crystallinity as function of temperature T, $K(T)$ is a cooling function of temperature, that is also called Ozawa crystallization rate constant, and m is Ozawa exponent depending on the crystal growth and nucleation mechanism. Equation 6 in the logarithmic form can be written as:

$$\log[-\ln(1 - X(T))] = \log K(T) - m\log\Phi. \tag{7}$$

Under the certain temperature, the Ozawa plots of $\log[-\ln(1 - X(T))]$ versus $\log \Phi$ for PP, PP-g-*m*-TMI, and PP-g-(St-*m*-TMI) are shown in Fig. 5. *m* and log $K(T)$ can be obtained from slope and intercept.

From these curves, it can be concluded that the $X(T)$ values calculated at various temperatures decrease with increasing cooling rate at a given temperature. The Ozawa method can successfully describe the non-isothermal crystallization process of PP, owing to the fact that the plots will give a series of lines for PP in Fig. 5a. However, for PP-g-*m*-TMI and PP-g-(St-*m*-TMI), the Ozawa plots show deviation from linearity under some temperatures, especially the curves of 396, 393, 392, and 389 K. Both the Avrami and the Ozawa methods failed to describe the non-isothermal crystallization kinetics of PP and its grafted products, which neglect the secondary crystallization. In order to better describe the overall process of nonisothermal crystallization of PP and its grafted product, Mo

Fig. 5 Ozawa plots of $\log[-\ln(1 - X(t))]$ versus $\log \Phi$ for crystallization of **a** PP, **b** PP-g-*m*-TMI and **c** PP-g-(St-*m*-TMI)
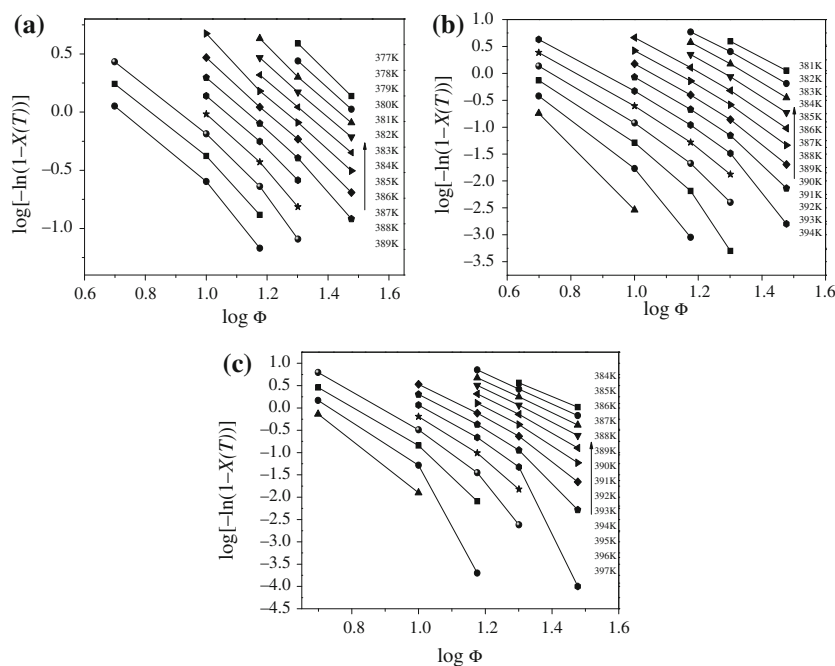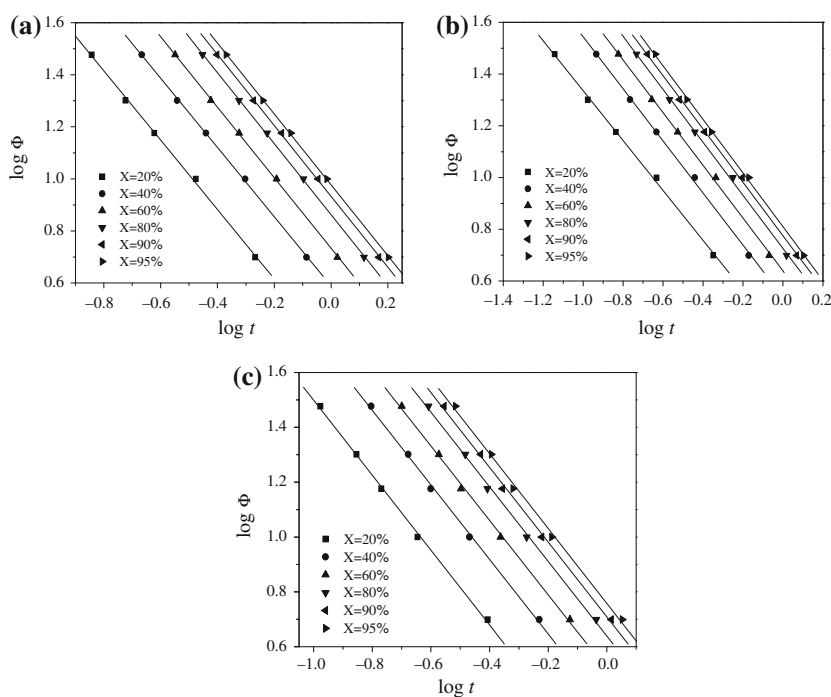
Fig. 6 Plots of log Φ versus log *t* for **a** PP, **b** PP-g-*m*-TMI and **c** PP-g-(St-*m*-TMI)

method [27] was tried. The kinetic equation was deduced by combining the Avrami equation with the Ozawa equation and thus a novel equation was obtained as follows:

$$\log\Phi = \log F(T) - \alpha\log t \tag{8}$$

where the parameter $F(T) = [K(T)/Z]^{1/m}$ refers to the value of cooling rate, which has to be chosen at unit crystallization time when the measured system amounts to a given crystallinity. This designates that $F(T)$ has a definite physical and practical meaning for non-isothermal crystallization process, as Z does for the isothermal case. α is the ratio of the Avrami exponent n to the Ozawa exponent m, i.e. $\alpha = n/m$. When selecting a certain relative crystallinity, from the plot of log Φ versus log *t* (Fig. 6), the values of α and $F(T)$ can be obtained by slopes and intercepts of fitting linear lines. The results are listed in Table 3.

It can be seen from Table 3 that value of α for neat PP varies from 1.33 to 1.36, from 0.96 to 1.04 for PP-g-*m*-TMI and from 1.35 to 1.36 for PP-g-(St-*m*-TMI). The variation in the values of α for three samples is small, indicating that the Mo method (Eq. 8) is successful in describing the non-isothermal process of PP, PP-g-*m*-TMI, and PP-g-(St-*m*-TMI). The values of $F(T)$ systematically increase with an increase in the relative crystallinity. At a given crystallinity, the higher the $F(T)$ value, the higher cooling rate is needed within unit crystallization time, indicating the difficulty of polymer crystallization. By comparing the values of $F(T)$ of different samples, we have found that $F(T)_{(PP-g-(St-m-TMI))} < F(T)_{(PP-g-m-TMI)} < F(T)_{(PP)}$, meaning that the crystallization rate of PP-g-(St-*m*-TMI) is fastest, and PP-g-*m*-TMI is faster than that of PP. This is in accordance with the result

obtained from the Avrami approach that the St and *m*-TMI act as nucleating agents and accelerate the crystallization of PP.

It is known that the crystallization of polymers is controlled by two factors: one is the dynamic factor, which is related to the activation energy for the transport of crystalline units across the phase and the other is the static factor that is related to the free energy barrier for nucleation. Considering the variation of T_p with cooling rate (Φ), the activation energy ΔE of non-isothermal crystallization can be evaluated from Kissinger method [28].

$$\frac{d[\ln(\Phi/T_p^2)]}{d(1/T_P)} = -\frac{\Delta E}{R} \tag{9}$$

where T_p, R, and Φ are the peak temperature, gas constant, and cooling rate, respectively. The crystallization activation energy is closely related to crystallization process, and can exhibit the crystallization ability being high or not (the higher ΔE value, the lower crystallization ability). Figure 7 shows the plots based on the Kissinger method, the slope of a plot of $\ln[\Phi/(T_p)^2]$ versus $1/T_p$ will give the crystallisation activation energy.

The activation energy of non-isothermal crystallization of PP, PP-g-*m*-TMI, and PP-g-(St-*m*-TMI) are 236.98, 226.17, and 203.05 kJ mol⁻¹, respectively, which note the grafting of *m*-TMI on the PP decrease the activation energy barrier, the accession of St further reduces the crystallization activation energy, indicating that PP can crystallize more easily in PP-g-*m*-TMI and PP-g-(St-*m*-TMI) than pure PP. These results are in agreement with the experimental results observed above. In the previous study, under

Table 3 Nonisothermal crystallization kinetic parameters by Mo method

Sample	$x/\%$	$\log F(T)$	α	R
PP	20	0.349	1.332	0.999
	40	0.589	1.330	0.999
	60	0.733	1.355	0.999
	80	0.862	1.365	0.999
	90	0.932	1.363	0.999
	95	0.977	1.362	0.999
PP-g-m-TMI	20	0.312	0.964	0.999
	40	0.537	1.008	0.999
	60	0.640	1.018	0.999
	80	0.726	1.024	0.999
	90	0.776	1.030	0.999
	95	0.810	1.038	0.999
PP-g-(St-m-TMI)	20	0.132	1.366	0.999
	40	0.375	1.358	0.999
	60	0.518	1.357	0.999
	80	0.639	1.360	0.999
	90	0.708	1.364	0.999
	95	0.758	1.365	0.999

the same cooling rate, the half time of the crystallization ($t_{1/2}$) of PP-g-(St-m-TMI) and PP-g-m-TMI decreased, that the crystallization speeded, and the results of Kissinger equation further descript that the crystallization activation energy of the grafted products reduced. All in all, after St and m-TMI is grafted on PP, its crystallization process has played two effects, those are the promotion of nucleation and nuclei growth, these results confirm the conclusion discussed above.

Conclusions

The non-isothermal crystallization kinetics of PP, PP-g-m-TMI, and PP-g-(St-m-TMI) were investigated by means of DSC technique under different cooling rates. The kinetic studies suggest under the same cooling rate, the relation of the crystallization peak temperature of PP, and its grafted products are, $T_{p(PP-g-(St-m-TMI))} > T_{p(PP-g-m-TMI)} > T_{p(PP)}$, and the half time of the crystallization is $t_{1/2(PP-g-(St-m-TMI))} < t_{1/2 (PP-g-m-TMI)} < t_{1/2(PP)}$. The Avrami equation, the Ozawa method, and the Mo approach were used for describing the non-isothermal crystallization behavior. The Avrami equation and the Ozawa method were inapplicable to satisfactorily describe the whole non-isothermal crystallization progress of PP, PP-g-m-TMI, and PP-g-(St-m-TMI). However, the Mo method can successfully describe the non-isothermal crystallization behavior of the three samples. The activation energy for non-isothermal
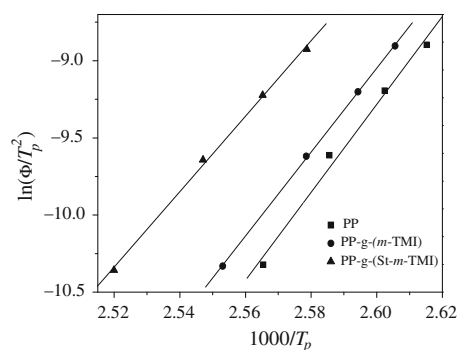
Fig. 7 The plots of $\ln(\Phi/T_p^2)$ versus $1/T_p$ of PP, PP-g-m-TMI and PP-g-(St-m-TMI)

crystallization of the three samples were determined by using Kissinger method, ΔE were estimated to be 236.98, 226.17, and 203.05 kJ mol^{-1} for neat PP, PP-g-m-TMI, and PP-g-(St-m-TMI), the lower value of activation energy for crystallization obtained for PP-g-m-TMI and PP-g-(St-m-TMI) confirmed the nucleating effect of St and m-TMI on crystallization of PP.

References

1. Seo Y, Kim J, Kim KU, Kim YC. Study of the crystallization behaviors of polypropylene and maleic anhydride grafted polypropylene. Polymer. 2000;41:2639–46.
2. Nur Y, Colak DG, Cianga I, Yagci Y, Hacaloglu J. Direct pyrolysis mass spectrometry studies on thermal degradation characteristics of poly(phenylene vinylene) with well-defined PSt side chains. J Therm Anal Calorim. 2008;94:157–62.
3. Yuan Q, Awate S, Misra RDK. Nonisothermal crystallization behavior of polypropylene-clay nanocomposites. Eur Polym J. 2006;42:1994–2003.
4. Ying JR, Liu SP, Guo F, Zhou XP, Xie XL. Non-isothermal crystallization and crystalline structure of PP/POE blends. J Therm Anal Calorim. 2008;91:723–31.
5. Hong HQ, He H, Jia DM, Ding C, Xu HX. Advances in polyolefins functionallization. Polym Eng Sci. 2006;22:623–7.
6. Braun D, Schmitt MW. Functionalization of poly(propylene) by isocyanate groups. Polym Bull. 1998;40:189–94.
7. Dexter RW, Saxon R, Fiori DE. m-TMI, a novel unsaturated aliphatic isocyanate. J Coat Technol. 1986;58:43–7.
8. Fu XJ, Xu Q, Jiang T. The role of styrene in isocyanate functionalization of ethylene-propylene copolymer. China Elastom. 2008;18:22–6.
9. Karmarkar A, Chauhan SS, Modak JM, Chanda M. Mechanical properties of wood–fiber reinforced polypropylene composites: effect of a novel compatibilizer with isocyanate functional group. Compos Part A Appl S. 2007;38:227–34.
10. Guo CG, Wang QW. Influence of m-isopropenyl-α, α-dimethylbenzyl isocyanate grafted polypropylene on the interfacial

interaction of wood-flour/polypropylene Composites. J Appl Polym Sci. 2008;109:3080–6.

11. Yin JH, Mo ZS. Modern polymer physics. Beijing: SciencePress; 2003.

12. Jiao CM, Wang ZZ, Liang XM, Hu Y. Non-isothermal crystallization kinetics of silane crosslinked polyethylene. Polym Test. 2005;24:71–80.

13. Stankowski M, Kropidłowska A, Gazda M, Haponiuk JT. Properties of polyamide6 and thermoplastic polyurethane blends containing modified montmorillonites. J Therm Anal Calorim. 2008;94:817–23.

14. Tao SP, Li ZM, Feng JM, Yang MB. Development progress of graft-modification functionalization of polyolefins. China Plast. 2002;16:1–5.

15. Janimak J, Cheng S, Zhang A, Hsieh E. Isotacticity effect on crystallization and melting in polypropylene fractions: 3. Overall crystallization and melting behaviour. Polymer. 1992;33:728–35.

16. Zhang CL, Feng LF, Xu ZB, Wang JJ, Gu XP. Study on the mechanism of melt-grafting of maleic anhydride and comonomer styrene onto polypropylene. J Funct Polym. 2005;18:373–7.

17. Zhu LC, Tang GB, Shi Q, Yin JH. Rare earth compounds assisted melt grafting of maleic anhydride onto isotactic polypropylene by reactive extrusion. Chem J Chin Univ. 2006;27:970–4.

18. Avrami M. Kinetics of phase change. II transformation-time relations for random distribution of nuclei. J Chem Phys. 1940;8:212–25.

19. Nagarajan K, Levon K, Myerson AS. Nucleating agents in polypropylene. J Therm Anal Calorim. 2000;59:497–508.

20. Wunderlich BI. Thermal characterization of polymeric materials. 2nd ed. New York: Academic Press; 1997.

21. Song B, Wang Y, Bai HW, Liu L, Li YL. Crystallization and melting behaviors of maleic anhydride grafted poly(propylene) nucleated by an aryl amide derivative. J Therm Anal Calorim. 2010;99:563–70.

22. Nath DCD, Bandyopadhyay S, Yu AB, Blackbum D, White C, Varughese S. Isothermal crystallization kinetics of fly ash filled iso-polypropylene composite and a new physical approach. J Therm Anal Calorim. 2010;99:423–9.

23. Zhang YF, Li X, Wei XS. Non-isothermal crystallization kinetics of isotactic polypropylene nucleated with 1,3:2,4-bis(3,4-dimethylbenzylidene) sorbitol. J Therm Anal Calorim. doi:10.1007/s10973-009-0372-1.

24. Zhang HF, Zhang QB, Sun CY. Nonisothermal crystallization kinetics of polypropylene/polyethersulfone blend. Polym Bull. 2008;60:291–300.

25. Li J, Zhou C, Wang G, Tao Y, Liu Q, Li Y. Isothermal and nonisothermal crystallization kinetics of elastomeric polypropylene. Polym Test. 2002;21:583–9.

26. Ozawa T. Kinetics of non-isothermal crystallization. Polymer. 1971;12:150–8.

27. Mo ZS. A method for the nonisothermal crystallization kinetics of polymers. Acta Polym Sin. 2008;7:656–60.

28. Kissinger HE. Variation of peak temperature with heating rate in differential thermal analysis. J Res Natl Bur Stand. 1956;57:217–21.